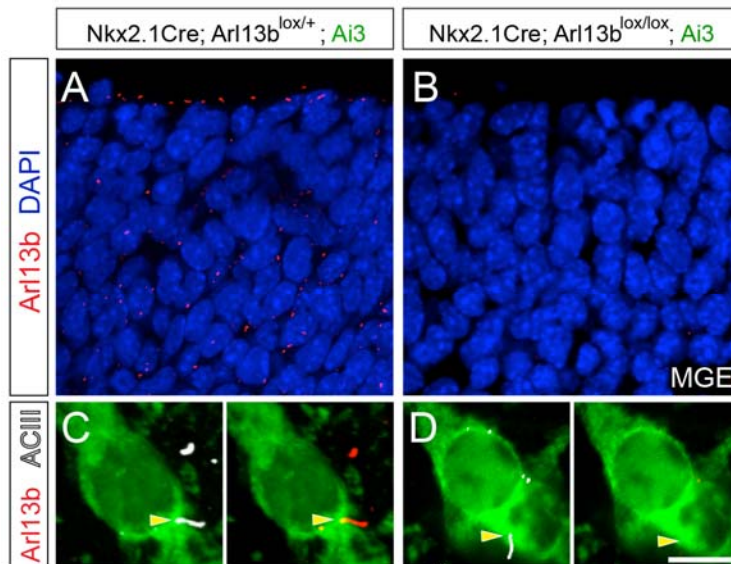


## Supplemental Figures and Legends

**Figure S1 (Related to Figure 1). Deletion of *Arl13b* in interneurons. (A-B)** Interneurons were labeled with anti-Arl13b antibodies (red) in *Nkx2.1Cre; Arl13b<sup>lox/+</sup>; Ai3* (A) and *Nkx2.1Cre; Arl13b<sup>lox/lox</sup>; Ai3* (B) brains [E14.5]. (C, D) Arl13b is absent in *Nkx2.1Cre; Arl13b<sup>lox/lox</sup>; Ai3* interneurons. Interneurons were co-labeled with anti-GFP, anti-Arl13b (red) and anti-ACIII (white) antibodies in *Nkx2.1Cre; Arl13b<sup>lox/+</sup>; Ai3* (C) and *Nkx2.1Cre; Arl13b<sup>lox/lox</sup>; Ai3* (D) brains. Arl13b is absent in the cilia (ACIII<sup>+</sup>) of *Nkx2.1Cre; Arl13b<sup>lox/lox</sup>; Ai3* interneurons (YFP<sup>+</sup>). Arrowheads (C, D) point to primary cilia. Scale bar, 20 $\mu$ m (A-B); 9 $\mu$ m (C-D).



**Figure S2 (Related to Figure 1 and Figure 2). Deletion of *Arl13b* results in cortical interneuron morphological and synaptic defects. (A, B)** YFP<sup>+</sup> interneurons in the neocortex of *Nkx2.1Cre; Arl13b<sup>lox/lox</sup>; Ai3* brains show reduced morphological complexity compared to control. Insets (A, B) show high magnification images of YFP<sup>+</sup> neurons. (C, D) Labeling with anti-PV antibodies show PV<sup>+</sup> interneuron morphological defects in the hippocampal dentate gyrus (DG) of *Nkx2.1Cre; Arl13b<sup>lox/lox</sup>* (D) mice [P30]. (E, F) Cortical interneurons were labeled with anti-PV or anti-GFP antibodies in *Nkx2.1Cre; Arl13b<sup>lox/+</sup>; Ai3* (E) and *Nkx2.1Cre; Arl13b<sup>lox/lox</sup>; Ai3* (F) brains. Cortical projection neurons were

counterstained with anti-NeuN antibodies. Arrowheads point to PV<sup>+</sup> or YFP<sup>+</sup> perisomatic synaptic boutons in control (E', E'') and mutant cortices (F', F''). (G, H) Quantification of PV<sup>+</sup>/YFP<sup>+</sup> perisomatic bouton density (G) and size (H) in control and *Nkx2.1Cre; Arl13b<sup>lox/lox</sup>; Ai3* cortices. Data shown are mean  $\pm$  SEM. \**P*<0.05 (Student's *t*-test,  $p_{[G]} = 0.0001$ ,  $p_{[H]} = 0.0001$ ). 42 cells from 4 different brains per group were analyzed. Scale bar, 88 $\mu$ m (A-B); 20 $\mu$ m (C-D); 12 $\mu$ m (E-F); 5.8 $\mu$ m (E', E'', F', F'').

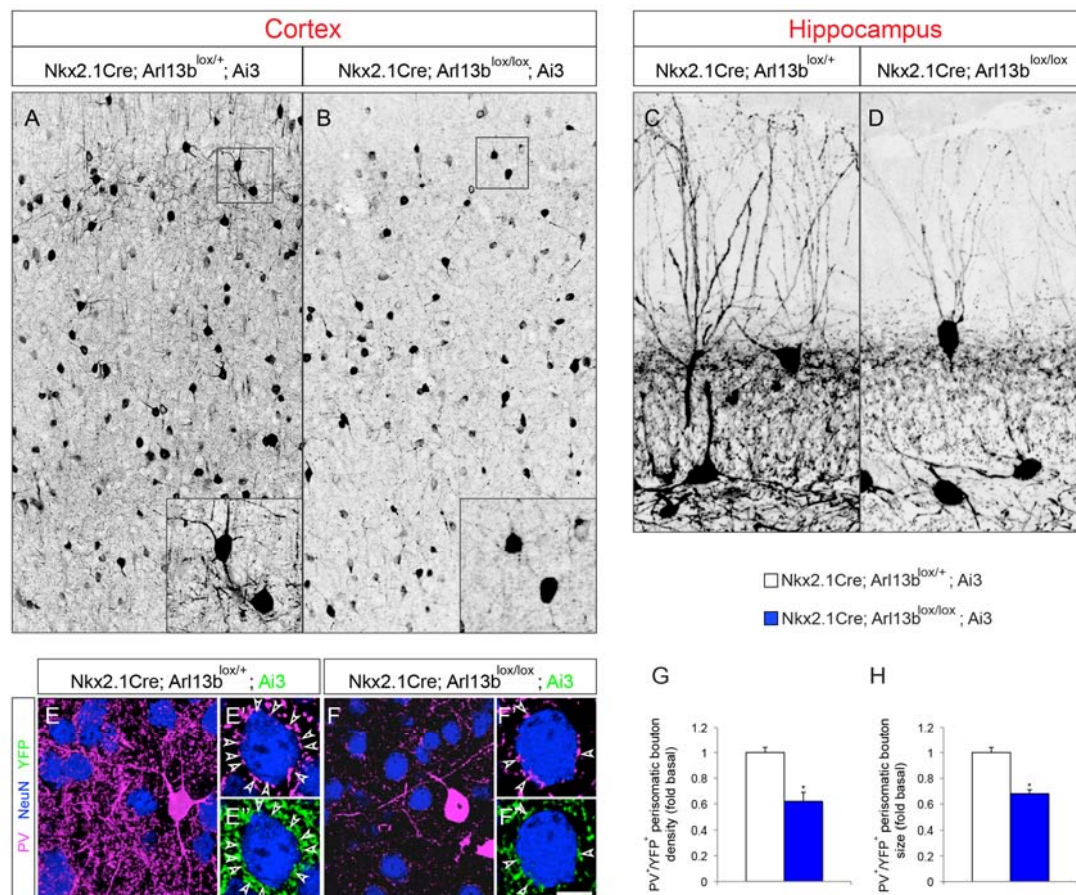


**Figure S3 (Related to Figure 1 and Figure 2). Deletion of *Arl13b* in postnatal PV<sup>+</sup> interneurons results in cortical interneuron morphological and synaptic defects.** (A-B) Co-labeling with anti-Arl13b (green) and anti-ACIII (blue) antibodies in the *ParvCre; Arl13b<sup>lox/+</sup>; Ai9* (A) and *ParvCre; Arl13b<sup>lox/lox</sup>; Ai9* (B) brains show loss of Arl13b in the cilia (arrowhead) of *ParvCre; Arl13b<sup>lox/lox</sup>; Ai9* interneurons. (C-F) TdTom<sup>+</sup> PV interneurons in the cortex (D) and hippocampal CA1 (F) region

of *ParvCre; Arl13b<sup>lox/lox</sup>; Ai9* brains show reduced morphological complexity compared to *ParvCre; Arl13b<sup>lox/+</sup>; Ai9* (C, E) brains [P60]. (G-H) Arrowheads point to tdTom<sup>+</sup> perisomatic synaptic boutons in *ParvCre; Arl13b<sup>lox/+</sup>; Ai9* (G) and *ParvCre; Arl13b<sup>lox/lox</sup>; Ai9* (H) cortices [P60]. Cortical projection neurons were counterstained with anti-NeuN antibodies. (I, J) Quantification of tdTom<sup>+</sup> perisomatic bouton (arrowhead) density (I) and size (J) in control and *ParvCre; Arl13b<sup>lox/lox</sup>; Ai9* cortices. Data shown are mean  $\pm$  SEM. \**P*<0.05 (Student's *t*-test, *p* = 0.0001). 22 cells from 4 different brains per group were analyzed. Scale bar, 11.8 $\mu$ m (A-B); 52 $\mu$ m (C-F); 5 $\mu$ m (G-H).

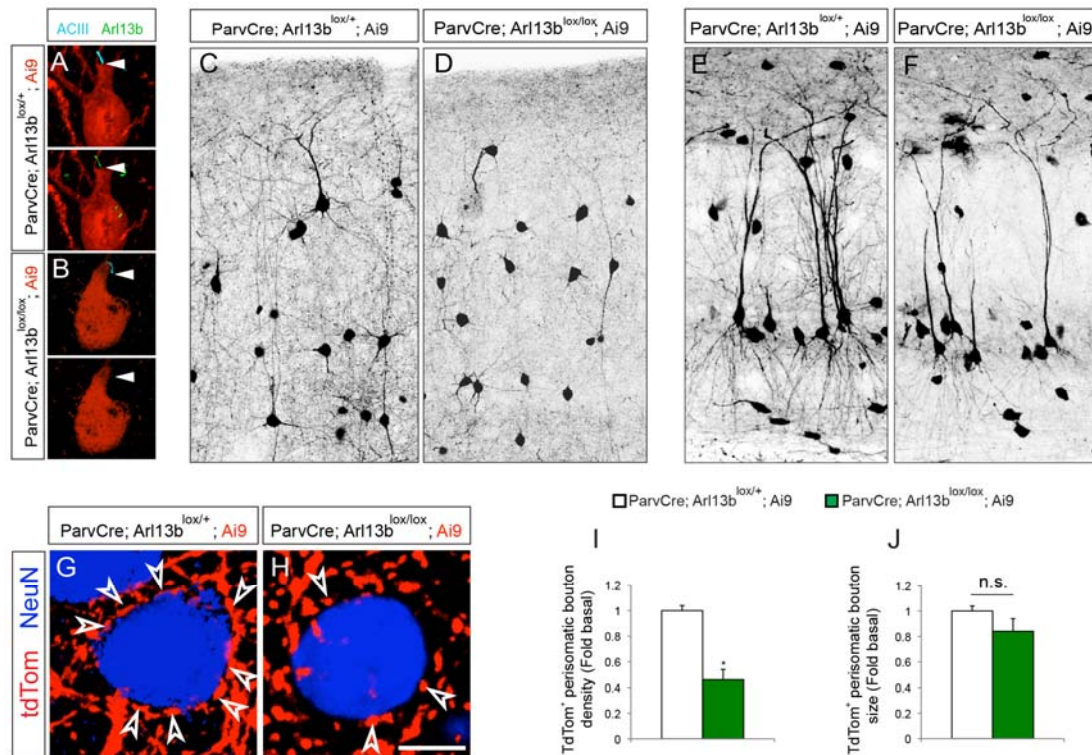


**Figure S4 (Related to Figure 2). Morphological and synaptic defects of Arl13b deficient interneurons *in vitro*.** (A-B) Dissociated interneurons from *Nkx2.1Cre; Arl13b<sup>lox/+</sup>; Ai9* (A) and *Nkx2.1Cre; Arl13b<sup>lox/lox</sup>; Ai9* (B) brains [E14.5] were cultured for 4 weeks and labeled with anti-VGAT antibodies. (A', B') Representative high-magnification images of VGAT<sup>+</sup> inhibitory presynaptic boutons along control (A') and Arl13b deficient (B') tdTom<sup>+</sup> interneuron axons. (C, D) Quantification of VGAT<sup>+</sup>

bouton density (C) and size (D) along control and mutant interneuron axons. Data shown are mean  $\pm$  SEM. 12 cells per group from 3 independent experiments were analyzed. \* $P < 0.05$  (Student's  $t$ -test,  $p_{[C]} = 0.003$ ,  $p_{[D]} = 0.01$ ). Scale bar, 20 $\mu$ m (A-B); 4.7 $\mu$ m (A'-B').

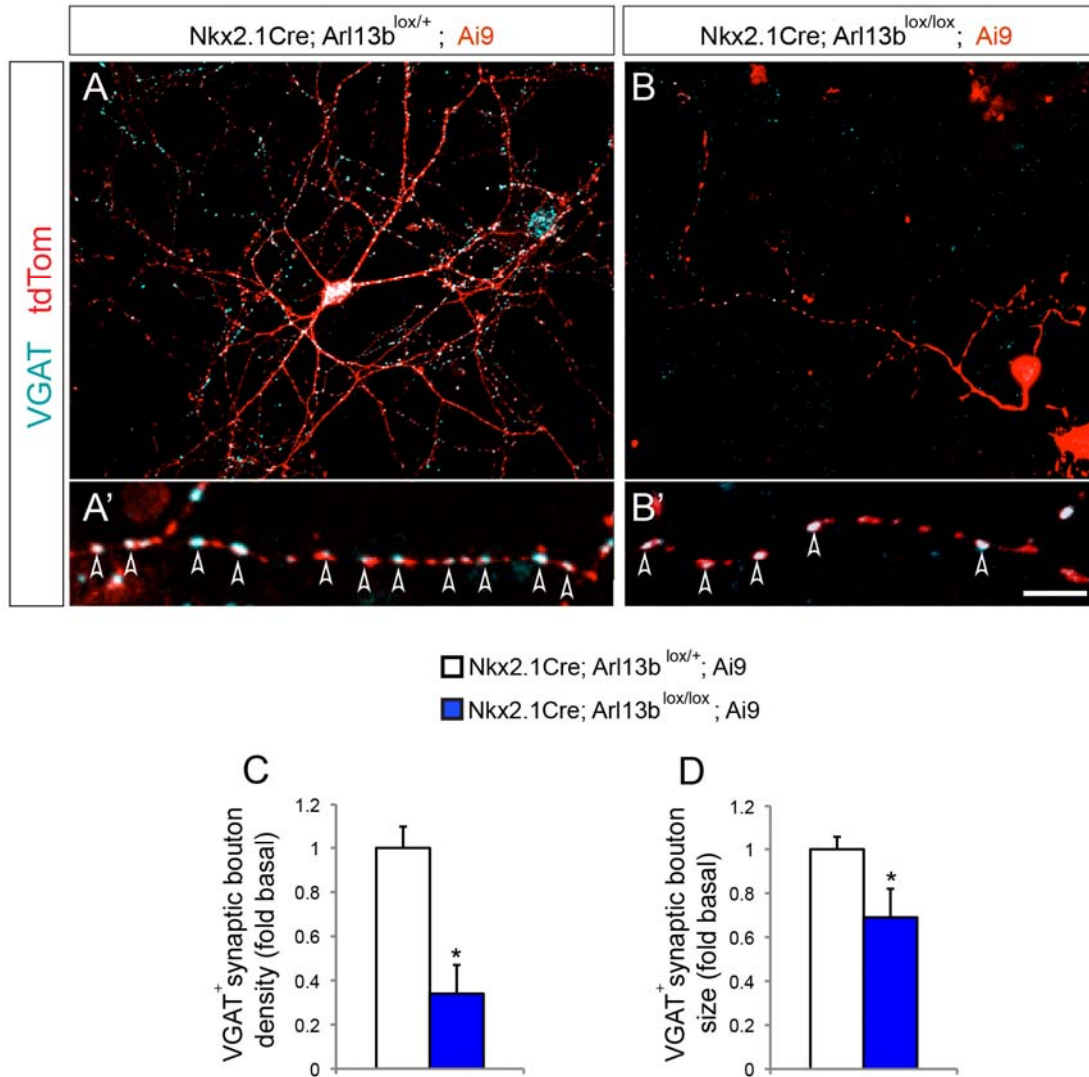


**Figure S5 (Related to Figure 5). Induced expression of Sstr3 in Arl13b deficient primary cilia rescues interneuron defects *in vitro*.** (A-C) Dissociated tdTom<sup>+</sup> INs from *Nkx2.1Cre; Arl13b<sup>lox/+</sup>; Ai9* (A), *Nkx2.1Cre; Arl13b<sup>lox/lox</sup>; Ai9* (B), *Nkx2.1Cre; Arl13b<sup>lox/lox</sup>; Sstr3-GFP; Ai9* and (D) *Nkx2.1Cre; Arl13b<sup>lox/lox</sup>; Ai9 + D124E-Sstr3* brains were cultured for 3 weeks. Inset (C-D) shows high-

magnification images of Sstr3-GFP (C) and D124E-Sstr3 (D) expression in primary cilium (arrowhead). (A'-D') Axons of tdTom<sup>+</sup> interneurons were co-labeled with anti-VGAT antibodies. Arrowheads point to VGAT<sup>+</sup> synaptic boutons along tdTom<sup>+</sup> axons. (E, F) Quantification of VGAT<sup>+</sup> synaptic bouton density (E) and size (F) in tdTom<sup>+</sup> interneuron axons. Data shown are mean  $\pm$  SEM. \* $P < 0.05$  (One-way ANOVA:  $F_{3,116} [E] = 47.3$ ;  $p_{[E]} = 4.8E-20$ ; post-hoc  $p_{[E, lox/+ \text{ vs. } lox/lox]} = 3.1E-13$ , post-hoc  $p_{[E, lox/lox \text{ vs. } lox/lox-Sstr3]} = 6.5E-10$ , post-hoc  $p_{[E, lox/lox \text{ vs. } lox/lox-D124E-Sstr3]} = 0.82$ ;  $F_{3,116} [F] = 24.1$ ;  $p_{[F]} = 3.3E-12$ ; post-hoc  $p_{[F, lox/+ \text{ vs. } lox/lox]} = 2.94E-08$ , post-hoc  $p_{[F, lox/lox \text{ vs. } lox/lox-Sstr3]} = 1.97E-07$ , post-hoc  $p_{[F, lox/lox \text{ vs. } lox/lox-D124E-Sstr3]} = 0.34$ ). Number of cells per group = 30. Scale bar, 20 $\mu$ m (A-D); 5 $\mu$ m (A'-D').

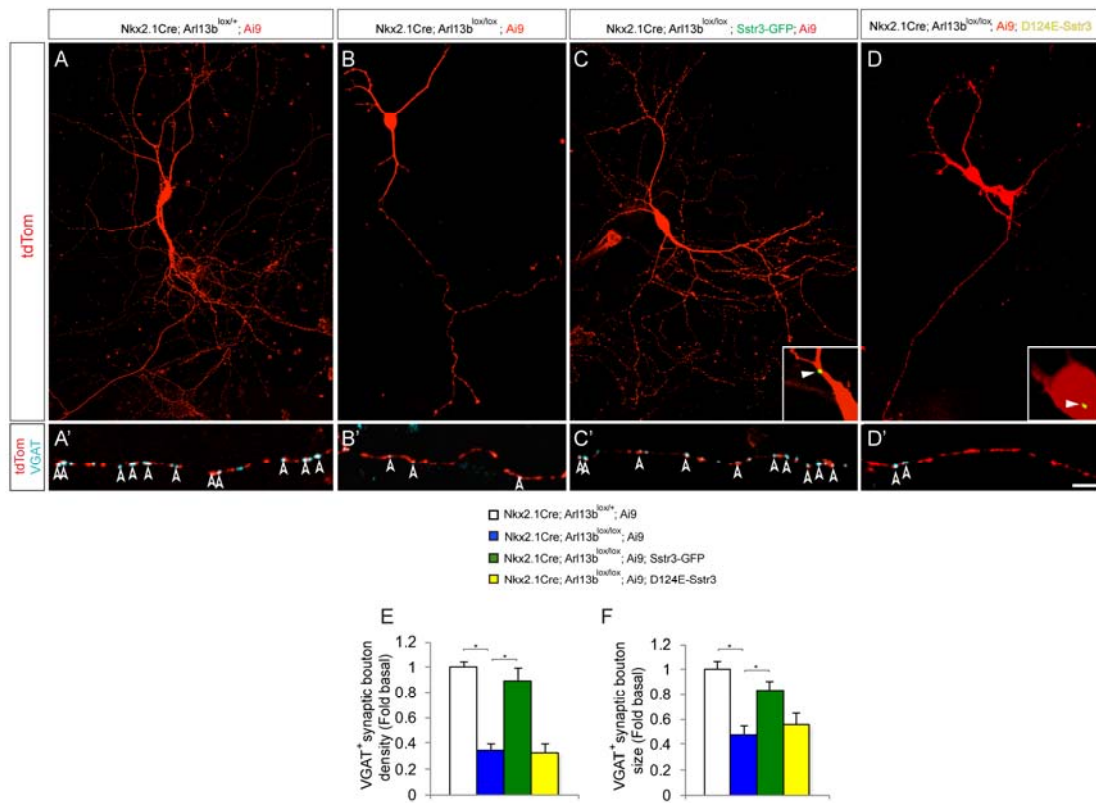
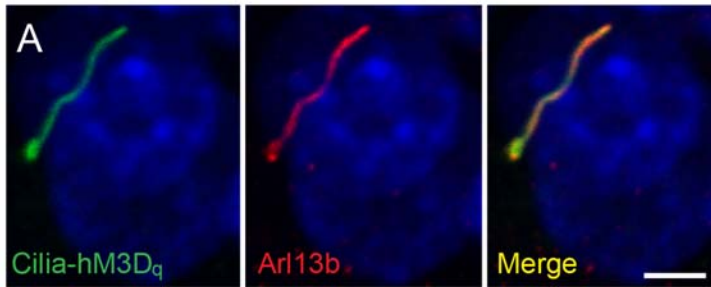


**Figure S6 (Related to Figure 6). Cilia-targeted expression of hM3D<sub>q</sub> DREADD.**

(A) Wild type MEFs were transfected with Cilia-hM3D<sub>q</sub> and labeled with anti-GFP and anti-Arl13b antibodies. Nuclei were counterstained with DAPI. (B) DREADD (GFP<sup>+</sup>) ratio in cilia vs. cytosol was measured and used as cilia localization index. The expression of Cilia-hM3D<sub>q</sub> is highly enriched in primary cilium. Data shown are

mean  $\pm$  SEM. (C) Cilia-hM3D<sub>q</sub> expression did not significantly affect ciliary length when compared to control cells. Data shown are mean  $\pm$  SEM. (Student's *t*-test, *p* > 0.05). Number of cells per group =16. Scale bar, 2.5 $\mu$ m.



□ Control  
■ Cilia-hM3D<sub>q</sub>

